JOURNAL OF GEOPHYSICAL RESEARCH, VOL. 104, NO. D24, PAGES 31,599–31,610, DECEMBER 27, 1999

Evidence of dynamic scaling in space-time rainfall

V. Venugopal[1], Efi Foufoula-Georgiou, and Victor Sapozhnikov

St. Anthony Falls Laboratory, Department of Civil Engineering, University of Minnesota, Minneapolis.

Abstract. As in any evolving process, including rainfall, variability in space and time are not independent of each other but depend in a way particular to the process at hand. Understanding and quantifying the space-time dependences in a process over a range of scales is not always easy because these dependences may be hidden under complex patterns with pronounced statistical variability at all scales. In this paper, we report our efforts to understand the spatiotemporal organization of rainfall at a range of scales (2 km to 20 km in space and 10 min to several hours in time) and explore the existence of simple relationships which might connect the rate of rainfall pattern evolution at small space and time scales to that at larger scales. Specifically, we seek to understand whether there exist space-time transformations under which these relationships can be parameterized in a simple scale-invariant framework. On the basis of analysis of several tropical convective storms in Darwin, Australia, we found that the rate of evolution of rainfall remains invariant under space-time transformations of the form $t \sim L^z$ (dynamic scaling). In other words, the dependence of the statistical structure of rainfall on space (L) and time (t) can be reduced to a single parameter t/L^z, where z is called the dynamic scaling exponent. The space-time organization in rainfall, apart from being interesting in its own right, permits the development of simple rainfall downscaling schemes which incorporate both spatial and temporal persistence.

1. Introduction

Many studies [e.g., *Gupta and Waymire*, 1990; *Schertzer and Lovejoy*, 1987; *Tessier et al.*, 1993; *Kumar and Foufoula-Georgiou*, 1993a, b; *Over and Gupta*, 1994] (see also *Foufoula-Georgiou and Krajewski* [1995] for a review and further references) have demonstrated the presence of a scale-invariant organization in spatial precipitation fields and have explored it for process understanding, relation of statistical to physical descriptions and development of efficient rainfall downscaling schemes. Temporal rainfall variability has also been studied for the presence of scale-invariance [e.g., *Olsson et al.*, 1993; *Veneziano et al.*, 1996; *Svensson et al.*, 1996; *Kumar*, 1996; *Cârsteanu and Foufoula-Georgiou*, 1996; *Venugopal and Foufoula-Georgiou*, 1996; *Cârsteanu*, 1997]. As in any evolving process, including rainfall, scales of variability in space and time are not independent of each other but relate in a way that might depend on the mechanism producing the storm. If, for example, a frozen field was advected with a constant velocity (without any other distortion), then spatial and temporal scales of variation would be simply related to each other via the advection velocity; that is, $L = Ut$. Such an evolution is hardly the case for complex natural processes, including rainfall, at least outside the range where some evidence for the presence of Taylor's hypothesis of turbulence has been suggested [e.g., *Zawadzki*, 1973].

Thus an important problem remains, the development of a framework which enables one to study simultaneously space and time organization of rainfall. If this framework is valid over a range of scales, then it is especially useful, because it allows one to predict the small-scale space-time rainfall variability from the larger-scale variability which is typically available from the output of a mesoscale model or from observations of a remote sensing device. The issue of studying spatiotemporal organization of precipitation at a range of scales has been recently tackled by *Over and Gupta* [1996] and *Marsan et al.* [1996]. *Over and Gupta* [1996] proposed a space-time rainfall model based on a multiplicative cascade in space and a Markovian evolution of the cascade weights in time. *Marsan et al.* [1996] proposed a space-time multifractal model based on a three-dimensional anisotropic multiplicative cascade. Both models start with specific choices of scaling,

[1]Now at Center for Ocean-Land-Atmosphere Studies, Calverton, Maryland.

Paper number 1999JD900437
0148-0227/99/1999JD900437$09.00

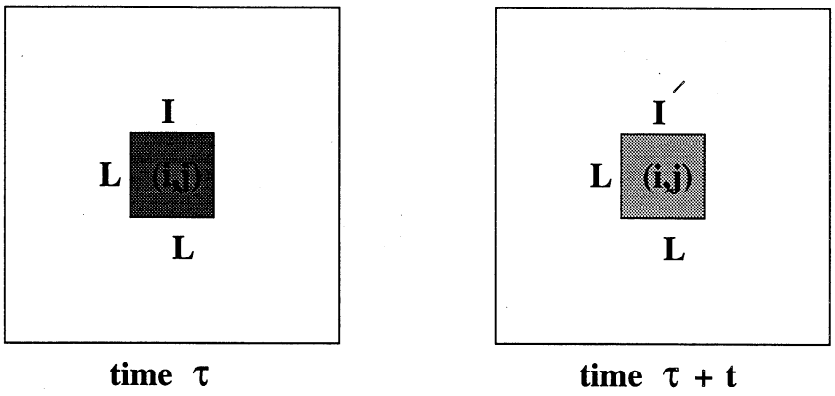

Figure 1. Schematic illustrating the change in intensity of a field (rainfall in this case) over a box of size $L \times L$ (spatial scale L) centered around the location (i, j) during a time interval t.

different from each other, and reproduce fairly well the spatiotemporal structure of rainfall.

In this paper, we propose a much simpler framework for analyzing simultaneously the space and time rainfall variability at a range of scales and parameterizing it in a way that is directly inferred from observations rather than imposed within a multiplicative cascade framework. Specifically, we sought to understand whether there exist space-time transformations under which relationships which connect the rainfall pattern evolution at small space-time scales to that at larger scales can be parameterized in a simple scale-invariant framework. We concentrated on the spatiotemporal organization of rainfall at the range of scales of 2 km to 20 km in space and 10 min to several hours in time, as these scales could be resolved from the available single-radar data.

2. Framework of Analysis

Consider a spatially variable field that evolves over time. We focus our attention on a particular location (i, j) of the field and study its evolution at that location by measuring how much the intensity of the field, at that location, has changed from time instant τ to time instant $\tau + t$, i.e., over a time lag t (see Figure 1). Now let us introduce a spatial scale parameter L and pose the question as to how much the intensity of the field, averaged over a box of size $L \times L$ centered around the location (i, j), changed during a time interval t (I to I' in Figure 1).

By studying this change over different spatial and temporal scales, one can get an idea of the statistical structure of the evolution of the field at multiple space and time scales. An issue that is of interest is to explore possible ways of rescaling space and time such that the spatiotemporal structure of the field remains statistically invariant. For that, we look for transformations that relate the dimensionless quantities t_1/t_2 (ratio of temporal scales) to L_1/L_2 (ratio of spatial scales), i.e., $t_1/t_2 = f(L_1/L_2)$, because the resulting framework would have the advantage of not being bound to a (arbitrary) measuring unit. The only such transformation f, as shown below, is a power law. If

$$\frac{t_1}{t_2} = f\left(\frac{L_1}{L_2}\right); \quad \frac{t_2}{t_3} = f\left(\frac{L_2}{L_3}\right)$$

$$\Longrightarrow \frac{t_1}{t_3} = \frac{t_1}{t_2}\frac{t_2}{t_3} = f\left(\frac{L_1}{L_2}\right) f\left(\frac{L_2}{L_3}\right);$$

but

$$\frac{t_1}{t_3} = f\left(\frac{L_1}{L_3}\right) = f\left(\frac{L_1}{L_2}\frac{L_2}{L_3}\right).$$

Thus

$$f\left(\frac{L_1}{L_2}\frac{L_2}{L_3}\right) = f\left(\frac{L_1}{L_2}\right) f\left(\frac{L_2}{L_3}\right)$$

$$\Longrightarrow f(L) = L^z,$$

i.e., a power law.

A spatiotemporal organization of such a nature in a process, i.e., the statistical invariance of a measure of evolution of the process under space-time transformations of the type $t \sim L^z$, is commonly referred to in the literature as "dynamic scaling" [*Czirok et al.*, 1993; *Kardar et al.*, 1986]. In other words, the presence of dynamic scaling in a process would imply that the dependence of the process on spatial scale L and on time t can be reduced to dependence on a single parameter t/L^z, where z is the so-called dynamical scaling exponent.

In the above discussion the evolution of the field was, for simplicity, measured by the change in intensity of the field over a time lag, i.e., by $(I' - I)$ in the short notation of Figure 1. This is applicable for a process that is additive, i.e., a process for which increments are independent of the intensity ($(I' - I) = \epsilon$, where ϵ is an independent identically distributed random variable). However, for a multiplicative process for which increments are dependent on the background intensity

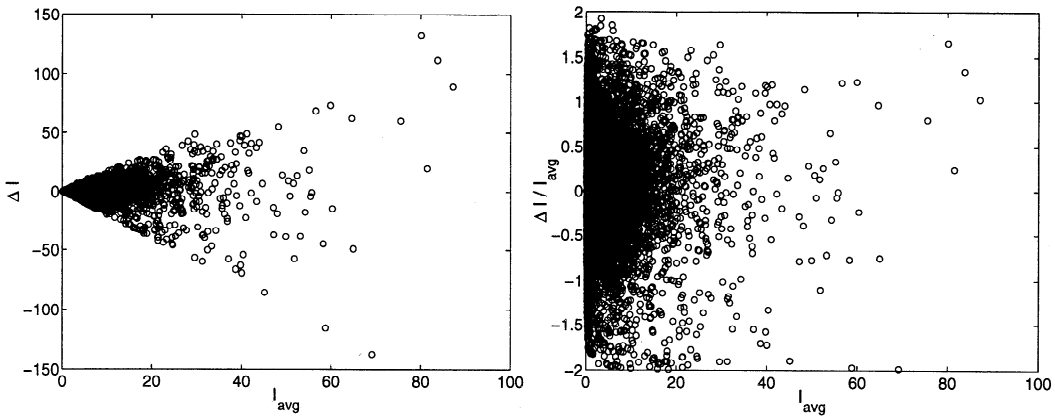

Figure 2. Evidence that normalized temporal rainfall fluctuations are independent of the background intensity. The plot on the left shows the temporal fluctuations of 2×2 km^2 rainfall intensities over 10 min (i.e., values $I^{'} - I$ at all pixels (i, j) in the schematic of Figure 1) as a function of the average rainfall intensity (i.e., $(I^{'} + I)/2$ in the terminology of Figure 1). A dependence of ΔI on I is apparent from this figure. If the fluctuations are normalized by the average intensity, this dependence is no longer present (plot on the right) and $(\Delta I/I)$ can be considered independent of I. These results are for the storm of January 4, 1994, in Darwin, Australia, but similar results were found for other storms.

$(I^{'}/I = \epsilon$ or $(I^{'} - I)/I = \epsilon^{'})$, it would be more appropriate to study the evolution of the log of the process, since log(process) is additive $(\ln I^{'} - \ln I = \epsilon^{''})$. Obviously, only the evolution of nonzero values of the field is studied in such a framework.

Thus, on the basis of evidence that relative changes in spatial rainfall fluctuations are independent of intensities [*Perica and Foufoula-Georgiou*, 1996], and that relative changes in temporal rainfall fluctuations are also independent of the background intensities (e.g., see Figure 2), we choose to measure rainfall evolution at a spatial scale L and time lag t by a statistical characterization of the field

$$\Delta \ln I_{i,j,\tau}(L,t) = \ln I^L_{i,j}(\tau + t) - \ln I^L_{i,j}(\tau) \qquad (1)$$

where $I^L_{i,j}(\tau)$ denotes the nonzero rainfall intensity at location (i, j), time instant τ, and spatial scale L. The parameter t represents the time lag over which the rainfall evolution is measured.

The measure described above is evaluated for all spatial locations (i, j), all time instants τ, and for various spatial and temporal scales, L and t, respectively. Then, assuming homogeneity in space (i.e., independence of the statistics of the process on the specific location (i, j)) and selecting regions in time where the statistics of $\Delta \ln I$ do not vary significantly around their mean value for that region, statistical characterization of $\Delta \ln I_{i,j,\tau}(L,t)$ at spatial scale L and temporal scale t is provided by the probability density function (PDF) of $\Delta \ln I(L,t)$. It is noted that the homogeneity in space is a reasonable assumption given that the radar frame can be seen as a fixed window within which the moving storm is observed. Thus unless there is a specific reason to believe that relative changes in rainfall intensities in a portion of the radar frame are much different than in another portion (note that we are considering the changes of nonzero rainfall only), a single probability density function can be assumed for the $\Delta \ln I$ values at all positions (i, j) of the frame. We also note here that the $\Delta \ln I$ fields are spatially uncorrelated (e.g., see Figure 3), so the PDFs of $\Delta \ln I(L,t)$ are sufficient to characterize the statistical structure of these fields at a range of scales. It is thus the statistical invariance of the PDF of $\Delta \ln I(L,t)$, under a space-time transformation of the type $t \sim L^z$ that we seek to explore.

The following gives an algorithmic approach toward the testing for the presence of dynamic scaling in rainfall:

1. $\Delta \ln I_{i,j,\tau}(L,t)$ is computed for various time lags, t (e.g., 10 min, 20 min, ...), and spatial scales, L (for instance, 2 km, 4 km, ...), at all (i, j) points of the field and for all time instants τ for which rainfall intensities are nonzero at both instants (τ and $\tau + t$), t units apart.

2. Periods in time are identified within which the statistical properties of $\Delta \ln I(L,t)$ do not depend significantly on the absolute time coordinate τ (see section 4.1 for details).

3. Within these periods, the PDFs of $\Delta \ln I(L,t)$ are evaluated for various time lags t and spatial scales L.

4. The PDFs of $\Delta \ln I(L,t)$ are checked to see if they remain statistically invariant under the space-time transformation, t/L^z = constant. (1) First, the second moments of the PDFs are checked to see if they remain invariant under that transformation. For that, pairs of t and L are found such that selected values of the second moments of the PDFs remain constant, and then the

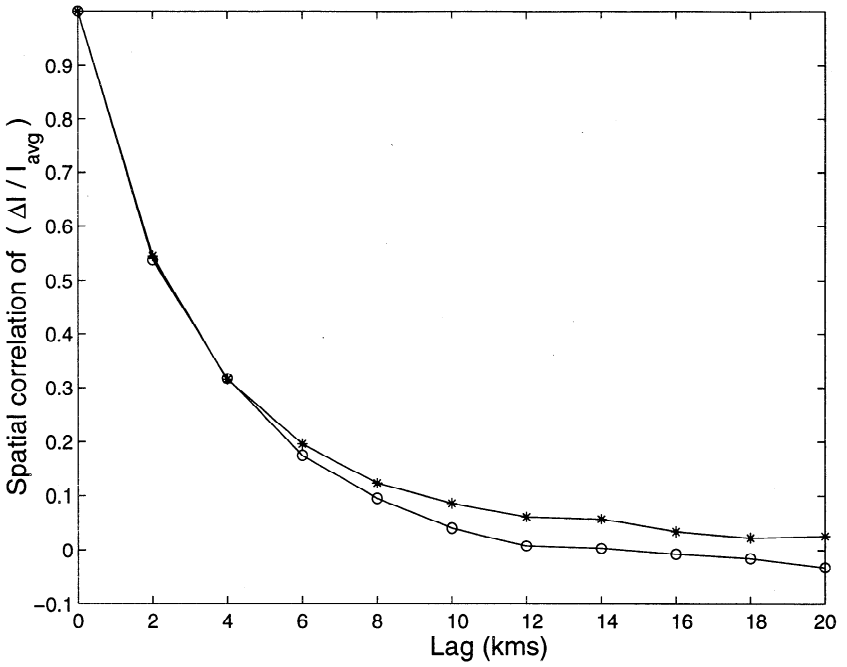

Figure 3. Evidence that normalized temporal rainfall fluctuations (here at a spatial scale 2 km and time lag of 10 min) are spatially uncorrelated. The circles represent the X correlation and the asterisks represent the Y correlation. This figure is for the January 4, 1994, storm over Darwin, Australia, but similar results were found for other storms.

corresponding iso-standard deviation lines are plotted on an L versus t plot. The log-log linearity of these lines suggests the presence of dynamic scaling. The slope of these lines, in turn, gives an estimate of the dynamic scaling exponent, z. (2) Using this value of z, the entire PDFs of $\Delta \ln I(L,t)$ are evaluated for the pairs of (t,L) corresponding to the iso-standard deviation lines and are checked to see if they remain statistically invariant under the above-mentioned transformation.

3. Data Sets Used in Analysis

The data used in our analysis were radar-depicted rainfall intensity fields at 2 km spatial resolution and 10 min temporal resolution, during the rainy season in Darwin, Australia. The conversion of radar reflectivities from a Doppler radar, which had a 5 cm wavelength and 1.65° beamwidth, to rainfall intensities was performed by R. Houze's group (personal communication, 1997) at the University of Washington. The storms we analyzed are those of December 28 and 30, 1993, and January 4, 1994. Figure 4 shows an instantaneous image of the storm of December 28, 1993, at 1741 UTC. The image (frame) is composed of 151 × 151 pixels, with each pixel representing rainfall over a 2 km area. For this storm, a total of 140 such frames, 10 min apart from each other (≈ 24 hours of storm duration), are available. Similar data are available for all other storms.

Figure 5 shows the variation of the mean intensity (mm/h), standard deviation of the rainfall intensity, and the percentage of nonzero pixels (i.e., the percentage of rain-covered area), over the total frame of 300 × 300 km^2 area, for the storms of December 28 and 30, 1993, and January 4, 1994. It is evident from these figures that these statistical properties change considerably over time, illustrating the temporal nonstationarity of the rainfall fields.

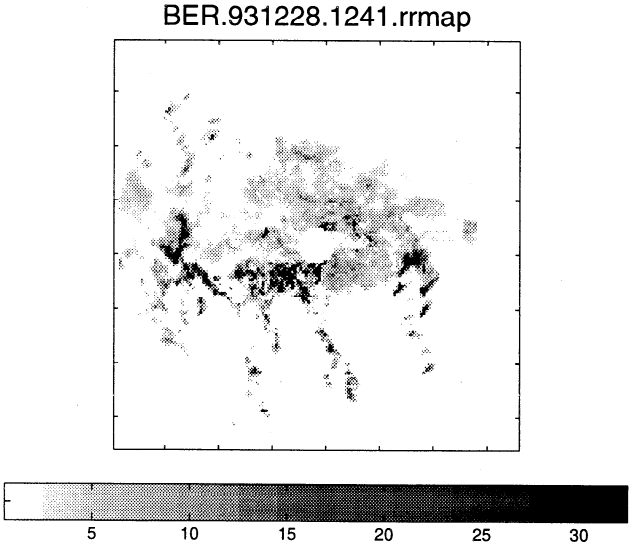

Figure 4. Radar-monitored rainfall field of December 28, 1993, in Darwin, Australia. The figure shows an instantaneous image of the storm at 1741 UTC. The total duration of the storm is approximately 24 hours (0500 UTC, December 28, 1993 to 0500 UTC, December 29, 1993). The intensities have been mapped onto 32 colors (see color bar) to avoid the high intensities masking the low intensities. The empty (circular) region in the middle was excluded from the analysis.

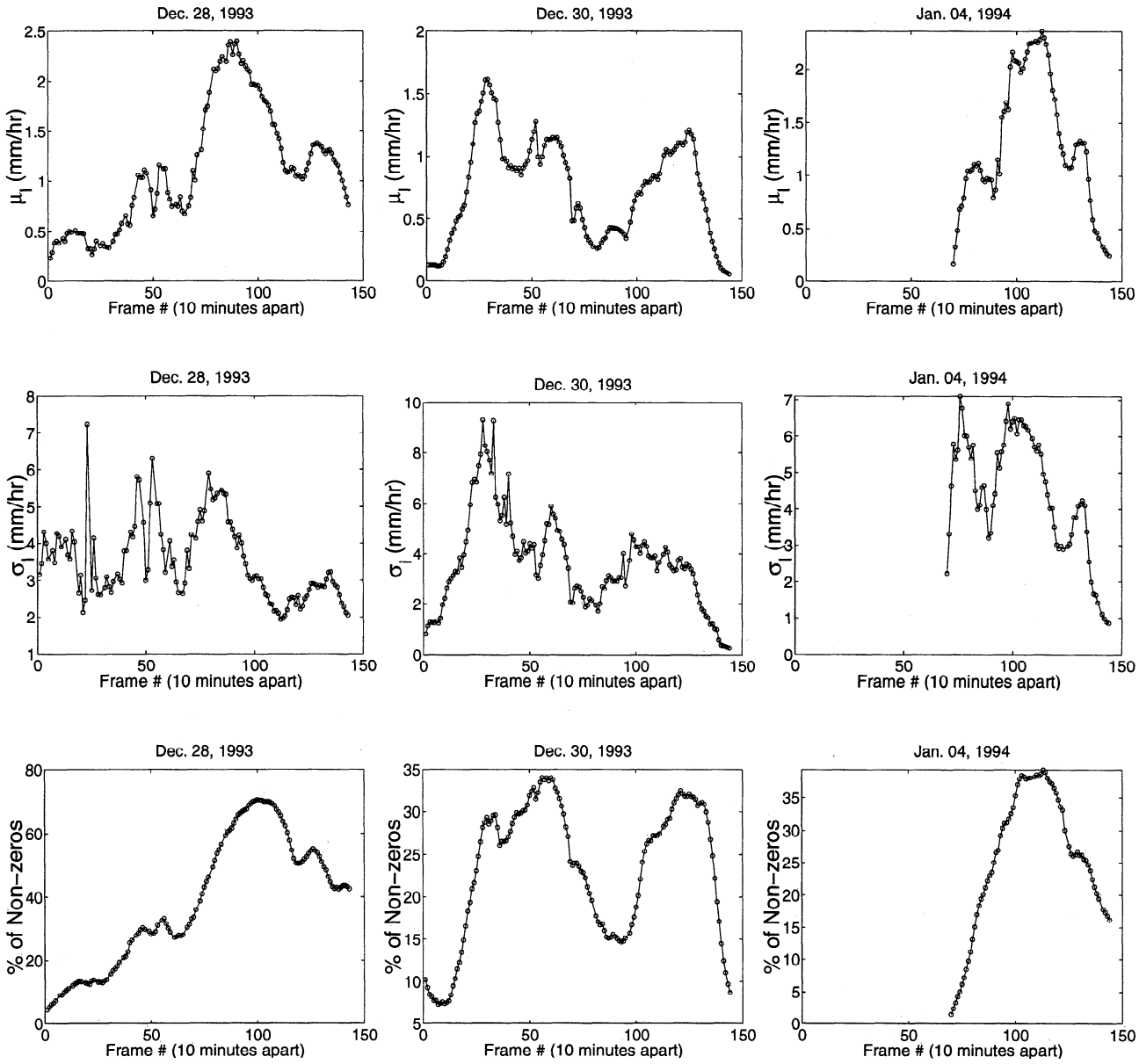

Figure 5. Temporal variation of the (a) mean, (b) standard deviation, and (c) percent of nonzero pixel values, for the radar-monitored rainfall field of December 28, 1993 (left column); December 30, 1993 (middle column), and January 4, 1994 (right column), in Darwin, Australia.

4. Analysis

4.1. "Stationarity" Considerations

In section 2 an algorithmic approach to test for the presence of dynamic scaling was presented. It was argued that $\Delta \ln I(L,t)$ can be assumed statistically homogeneous in space within the radar frame, and thus for a given spatial scale L and time lag t, a single PDF of $\Delta \ln I(L,t)$ can be used for the entire frame. However, independence of this PDF on absolute time cannot be assumed a priori. Thus the statistical moments of the PDF of $\Delta \ln I(L,t)$ must be checked to see how they might change over time. Then, the assumption that all $\Delta \ln I$ values come from the same probability distribution can be made only within those time periods over which the variation of the statistical moments of $\Delta \ln I$'s, around their mean values for these periods, is not significant.

It was found that the mean of $\Delta \ln I$ fluctuates, with time, around zero, with a variation of about 10-15% of the standard deviation of $\Delta \ln I$ (see Figure 6). On the other hand, the standard deviation of $\Delta \ln I$ shows a significant change with time, namely, a decreasing trend, as is seen from Figure 6. The presence of such a change in $\sigma(\Delta \ln I)$ poses the problem of identifying regions over which the variation of $\sigma(\Delta \ln I)$ around its mean value is not significant, such that a single PDF (for each time lag and spatial scale) can be assumed in that region.

To decide on whether $\sigma(\Delta \ln I)$ varies significantly in a region, two measures on $\sigma(\Delta \ln I)$ can be used: (1)

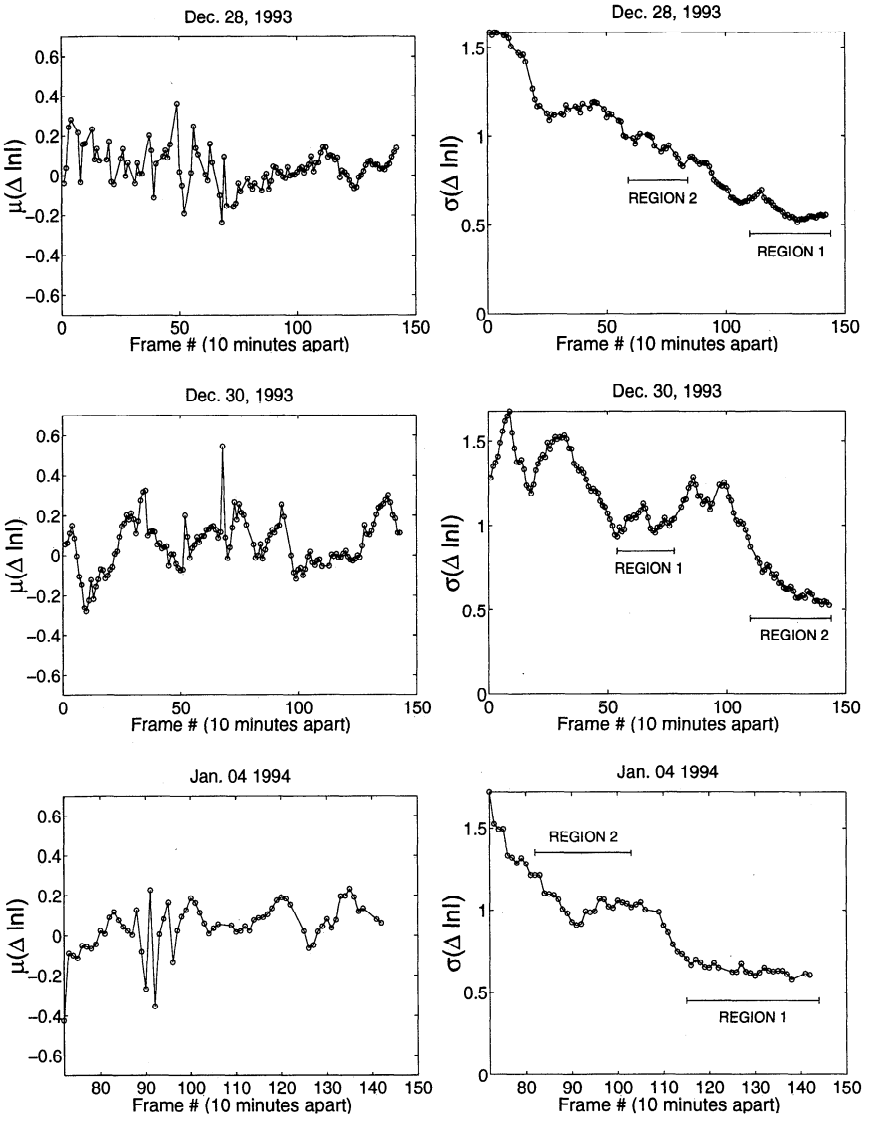

Figure 6. Temporal variation of the mean (left column) and standard deviation (right column) of $\Delta \ln I$ for temporal scale (time lag) $t = 10$ min and spatial scale $L = 2$ km for the storms of December 28 (top) and 30, 1993 (middle), and January 4, 1994 (bottom). This figure illustrates that the variability of the mean of $\Delta \ln I$ is small compared to that of the standard deviation of $\Delta \ln I$. Regions 1 and 2 indicate two regions where $\mu(\Delta \ln I)$ and $\sigma(\Delta \ln I)$ do not fluctuate significantly around their mean values for the region and thus were chosen for testing the presence of dynamic scaling in $\Delta \ln I$.

percentage of variation, i.e., (max - min)/average, and (2) spread, i.e., standard deviation, of $\sigma(\Delta \ln I)$. The latter measure is more stable than the former for the reason that the percentage of variation depends predominantly only on two values, i.e., the maximum and the minimum. Hence we choose the spread in $\sigma(\Delta \ln I)$ as our measure to decide if the second moment of $\Delta \ln I$ changes significantly over time. For instance, consider the top right plot in Figure 6 (for the storm of December 28, 1993). Region 1 has an average $\sigma(\Delta \ln I)$ equal to 0.57 and a spread of 0.05. In other words, the fluctuations in the standard deviation are small ($\approx 10\%$) compared to the average standard deviation in region 1, and hence it can be assumed that $\sigma(\Delta \ln I)$ does not vary significantly around its mean in that region. Using this criterion and a cutoff value of 15% in fluctuation around the mean value, several such regions (referred to as "stationary" regions) were identified for each storm. Some of these regions are shown in Figure 6.

4.2. Results

The dynamic scaling testing procedure elaborated in section 2 was then applied to several "stationary" regions of all three storms. Here a detailed discussion is presented for region 1 of the storm of December 28, 1993, and a summary of results is given for the other

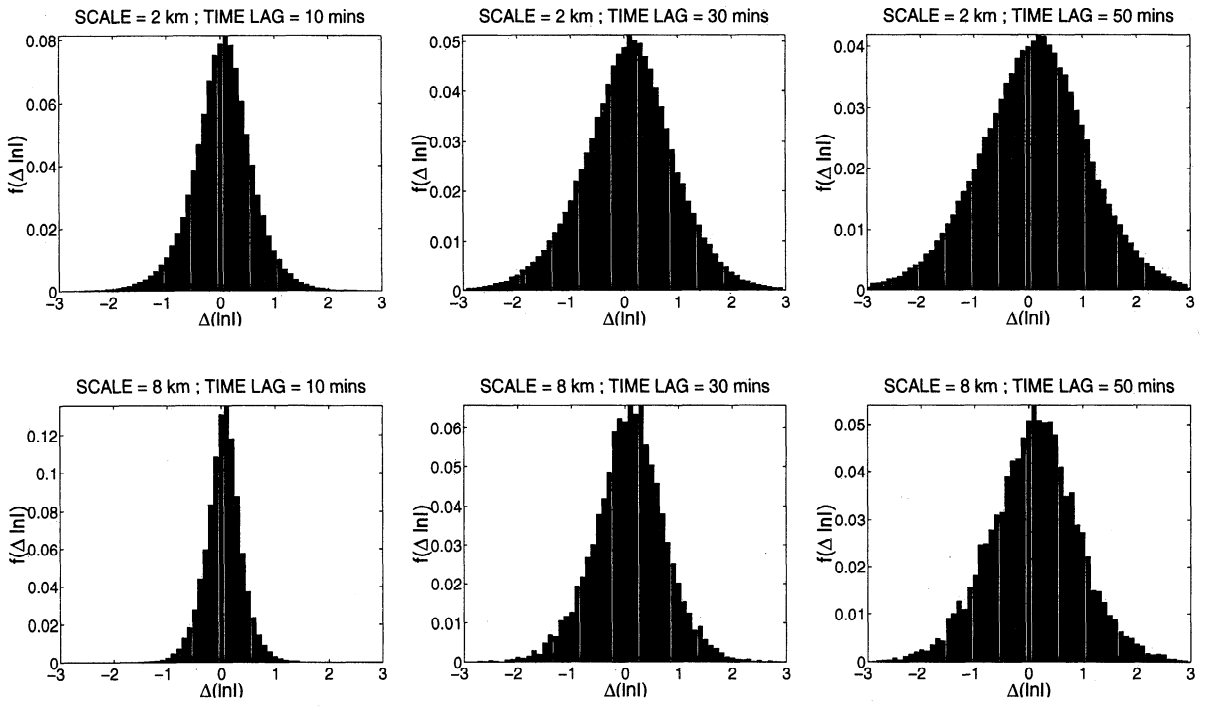

Figure 7. Selected PDFs of $\Delta \ln I$ (for spatial scales, 2 and 8 km, and time lags, 10, 30, and 50 min) for region 1 of the storm of December 28, 1993.

regions. The spatial (aggregation level) and temporal (time lag) scales at which $\Delta \ln I(L,t)$ is computed are 2, 4, 8, and 16 km, and 10, 20, 30, ..., 80 min, respectively. Figure 7 shows the PDFs of $\Delta \ln I(L,t)$ for selected spatial scales (2 and 8 km) and temporal scales (10, 30, and 50 min) for region 1 of the storm of December 28, 1993. As was expected, these PDFs are not identical but depend on the spatial and temporal scale. It is worth mentioning here that the PDFs of $\Delta \ln I(L,t)$ exhibit normality. This is consistent with the results of *Kedem et al.* [1990] who found log-normality in spatially averaged rainrates from GATE data under various space-time sampling designs.

Let $\Sigma(\Delta \ln I)(L,t)$ ($\Sigma(\Delta \ln I)$, in short) denote the standard deviation of the PDF formed from all values of $\Delta \ln I$ over a "stationary" region, e.g., region 1, at spa-

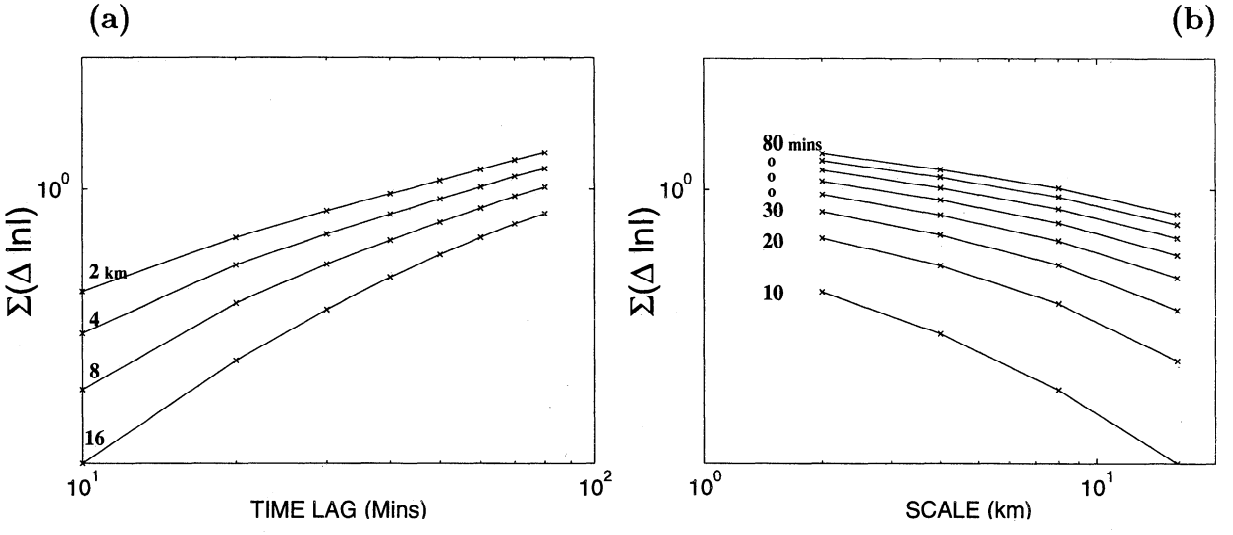

Figure 8. Plot indicating the lack of spatial and temporal simple scaling of $\Delta \ln I$ for the December 28, 1993, storm: (a) plot of $\Sigma(\Delta \ln I)$ for different spatial scales (bottom to top: 16, 8, 4, and 2) corresponding to time lags 10, 20, ..., 80 min; (b) plot of $\Sigma(\Delta \ln I)$ for different time lags (bottom to top: 10, 20, ..., 80 min) corresponding to spatial scales 2, 4, 8, and 16. The results shown here are from analysis of region 1. Lack of log-log linearity indicates the absence of spatial and temporal scaling in the standard deviations of $\Delta \ln I$.

Table 1. Standard Deviations of $\Delta \ln I$, $\Sigma(\Delta \ln I)$, With Time Lag (Left to Right) and Aggregation Level (Top to Bottom), for Region 1 of the Storm of December 28, 1993

	Time Lag t, min							
L, km	10	20	30	40	50	60	70	80
2	0.58	0.77	0.89	0.97	1.05	1.11	1.17	1.21
4	0.47	0.67	0.79	0.87	0.95	1.01	1.07	1.12
8	0.35	0.55	0.67	0.76	0.84	0.90	0.96	1.01
16	0.23	0.40	0.53	0.63	0.71	0.77	0.83	0.88

tial scale L and time lag t. Note that $\Sigma(\Delta \ln I)$ is different from $\sigma(\Delta \ln I)$, which is the instantaneous (at time instant τ) spatial standard deviation of $\Delta \ln I(L,t)$. (In fact, $\Sigma(\Delta \ln I) \approx \overline{\sigma(\Delta \ln I)}$, where the latter is the average value of $\sigma(\Delta \ln I)$ over the "stationary" region.) Figures 8a and 8b show the variation of the standard deviation $\Sigma(\Delta \ln I)$ of these PDFs with time lag and spatial scale, respectively. As anticipated, Σ increases with time lag for a given spatial scale (presumably, new, distinct features appear or existing patterns disappear with time) and decreases with aggregation level for a given time lag (since aggregation implies smoothing). The nonpower-law behavior (equivalently, the nonlinear behavior in a log-log plot) seen in the plots of Figure 8 indicates that $\Delta \ln I$ does not exhibit spatial or temporal scaling.

The values of $\Sigma(\Delta \ln I)$ for the various spatial scales L and time lags t, used to construct Figs. 8a and 8b, are displayed in Table 1 in a matrix form. From Table 1, one can (by linear interpolation) find pairs of L and t for which Σ remains constant. In other words, one would select a value of Σ and, for each spatial scale, evaluate by linear interpolation, from the table, the time corresponding to the chosen Σ. This is repeated for different values of Σ. (It is to be noted that the values of Σ chosen fall completely within the range of the values in the table of standard deviations as extrapolation should be avoided.) Table 2 gives, for example, pairs of t and L for which $\Sigma = 0.6$, 0.7, and 0.8. If these (L,t) pairs for every constant value of Σ are found to satisfy $t \sim L^z$, i.e., if they plot as straight lines (called iso-Σ lines) on a log-log plot, then it supports the hypothesis that rainfall evolution exhibits dynamic scaling. Figure 9, which is a plot of the values in Table 2, indeed shows log-log linearity of the iso-Σ lines and thus verifies the dynamic scaling hypothesis.

Table 2. Time (in min) to "Reach" Different Standard Deviations (Left to Right: 0.6, 0.7, 0.8) for Various Aggregation Levels (Top to Bottom), for Region 1 of the Storm of December 28, 1993

	$\Sigma(\Delta \ln I)$		
L, km	0.6	0.7	0.8
2	11.1	16.3	22.4
4	16.6	22.8	31.6
8	24.4	33.3	45.1
16	37.4	49.4	64.7

Pairs (L,t) = (2, 11.1), (4, 16.6), (8, 24.4), and (16, 37.4) give the same $\Sigma(\Delta \ln I) = 0.6$, and so on.

The value of z, the dynamic scaling exponent, is estimated from the slope of the iso-Σ lines. For example, from Figure 9 the minimum least-squares straight line fits give estimates of $z = [0.58, 0.54, 0.51]$ corresponding to $\Sigma = [0.6, 0.7, 0.8]$, respectively. These estimates of z are not significantly different from each other at the 95% significance level and for all practical purposes a single value of z can be assumed. This value can simply be the average of the three estimates of z or can be the estimate obtained from a single iso-Σ line corresponding to the mean value $\overline{\sigma(\Delta \ln I)}$ for that region. Note that in this region the fluctuations of σ around their mean value $\overline{\sigma}$ are not statistically significant, and thus a single iso-standard deviation line corresponding to $\overline{\sigma}$ suffices.

When the pairs (L,t) for which $\Sigma(\Delta \ln I)$ remains constant are found (see Table 2), the whole PDFs corresponding to these Σ values (and the corresponding z values) can be evaluated. This can be done by linearly interpolating the PDF ordinates that were computed for various temporal scales (t = 10, 20, ..., 80 min) and spatial scales (L = 2, 4, ..., 16 km) to the (L,t) pairs of constant $\Sigma(\Delta \ln I)$ shown in Table 2. For example, the ordinates of the PDF for (L,t) = (2 km, 11.1 min) corresponding to $\Sigma(\Delta \ln I) = 0.6$ (Table 2) are computed by linear interpolation of the ordinates of the known PDFs for (L,t) = (2 km, 10 min) and (L,t) = (2 km, 20 min). The same is done for all other iso-Σ pairs of (L,t). The similarity of these interpolated PDFs (see Figure 10) confirms that not only $\Sigma(\Delta \ln I)$ but also the whole PDFs of $(\Delta \ln I)$ remain statistically invariant under the transformation t/L^z = constant. It is worth mentioning here that from the presence of dynamic scaling in $\Sigma(\Delta \ln I)$, and the fact that the distributions of $\Delta \ln I$ are Gaussian with zero mean (see Figure 7), one could expect the statistical invariance of the whole PDFs too. Similar results were found for the other two storms. For example, Figure 11 shows that

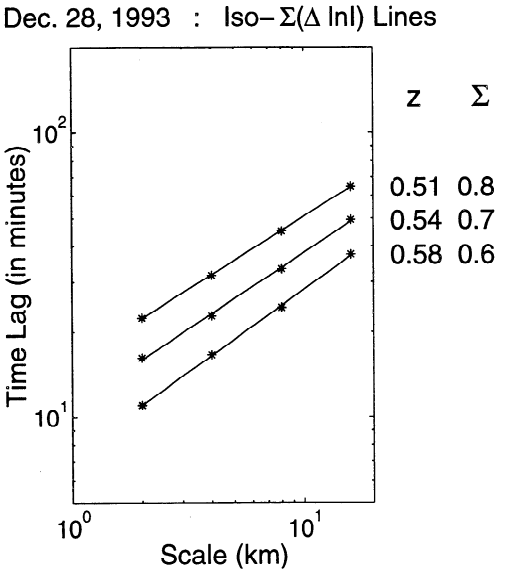

Figure 9. Plot illustrating the presence of dynamic scaling in the standard deviations of $\Delta \ln I$ for region 1 of the storm of December 28, 1993, in Darwin, Australia. The log-log linear relationship between t and L for values of $\Sigma(\Delta \ln I) = 0.8$, 0.7, and 0.6 (top to bottom), verifies the presence of dynamic scaling and gives estimates of the dynamic scaling exponent $z = 0.51$, 0.54, and 0.58, respectively.

dynamic scaling is present in the "stationary" regions (region 1) of the storms of December 30, 1993, and January 4, 1994,respectively.

Thus from the analysis of the three Darwin storms presented earlier, it is evident that there is dynamic scaling present in the proposed measure of rainfall evolution. Table 3 lists the values of z for all six "stationary" regions of the three storms shown in Figure 6. The single value of z reported here is the estimate obtained from the iso-standard deviation line corresponding to $\overline{\sigma(\Delta \ln I)}$ for the region. Note that the value of z falls in the range of 0.6-0.7 for four regions and is 0.8 and 1.2 for two regions. On further examination, the four regions that have the $z \in [0.6, 0.7]$ correspond to regions where the mean rainfall intensity and percentage-area covered by rain, decrease, i.e., the dissipation stage of the storm. On the other hand, the two regions where z was found to be 0.8 and 1.2 come from exactly the opposite scenario, namely, increasing mean rainfall intensity and percentage-area covered by rain, i.e., the buildup stage of the storm. This points to the possibility of the dependence of z on the dynamics of the storm since presumably the storm parameters associated with the dynamics of the buildup and dissipation stages of a storm are different. This issue needs to be further examined and many more storms analyzed to be able to understand the dependence of z to the storm dynamics.

To understand the significance of the value of z, let us consider $z = 0.6$. The presence of dynamic scaling tells us that

$$\frac{t_1}{t_2} = \left(\frac{L_1}{L_2}\right)^z.$$

This implies that the time (t_2) it takes for a feature of size 2×2 km^2 (L_2) to undergo the same evolution ($\Delta \ln I$), as what a feature of size 16×16 km^2 (L_1) would in time t_1, is

$$t_2 = t_1 \left(\frac{2}{16}\right)^{0.6} \approx 0.3 t_1;$$

that is, the rate of change of the 8-times smaller feature is 3 times faster than the larger feature. Note that the rate of evolution does not depend on the actual sizes of the two features but only on their ratio. Such a spatiotemporal organization in rainfall is interesting and is also useful in developing parsimonious space-time downscaling models. Such a model has been recently explored by the authors and is presented in a companion paper [*Venugopal et al.*, 1999].

5. Conclusions

Several studies have investigated the multiscale structure of rainfall separately in space and time or have imposed a particular structure in space and have inferred the one in time and vice versa. In this study, an attempt was made to study the multiscale spatiotemporal structure of rainfall simultaneously in space and time. In particular, we explored the existence of a space-time transformation such that rainfall evolution remained statistically invariant over a range of scales. It is emphasized that the impetus of our study was not to make inferences about the underlying physical mechanisms producing rainfall. Rather we were motivated by (1) the need to develop a simple framework under which spatial and temporal rainfall could be studied simultaneously without imposing model structures but allowing the data to indicate the underlying relationships, and (2) the hope that these relationships can aid in disaggregating large space-time scale rainfall fields (e.g., outputs of regional models) to smaller scales needed for water resources management studies.

The findings of this research suggest that there exists a space-time transformation of the power-law form $t \sim L^z$ under which rainfall evolution remains statis-

Table 3. Values of z for Different Regions of the Three Storms Described in Section 3

Storm Date	Region	$\overline{\sigma(\Delta \ln I)}$	Spread	z
December 28, 1993	1	0.57	0.05	0.6
	2	0.95	0.09	1.2
December 30, 1993	1	1.02	0.05	0.7
	2	0.63	0.08	0.6
January 4, 1994	1	0.65	0.4	0.6
	2	1.02	0.05	0.8

Spread is the standard deviation of $\sigma(\Delta \ln I)$ around the mean value of $\overline{\sigma(\Delta \ln I)}$.

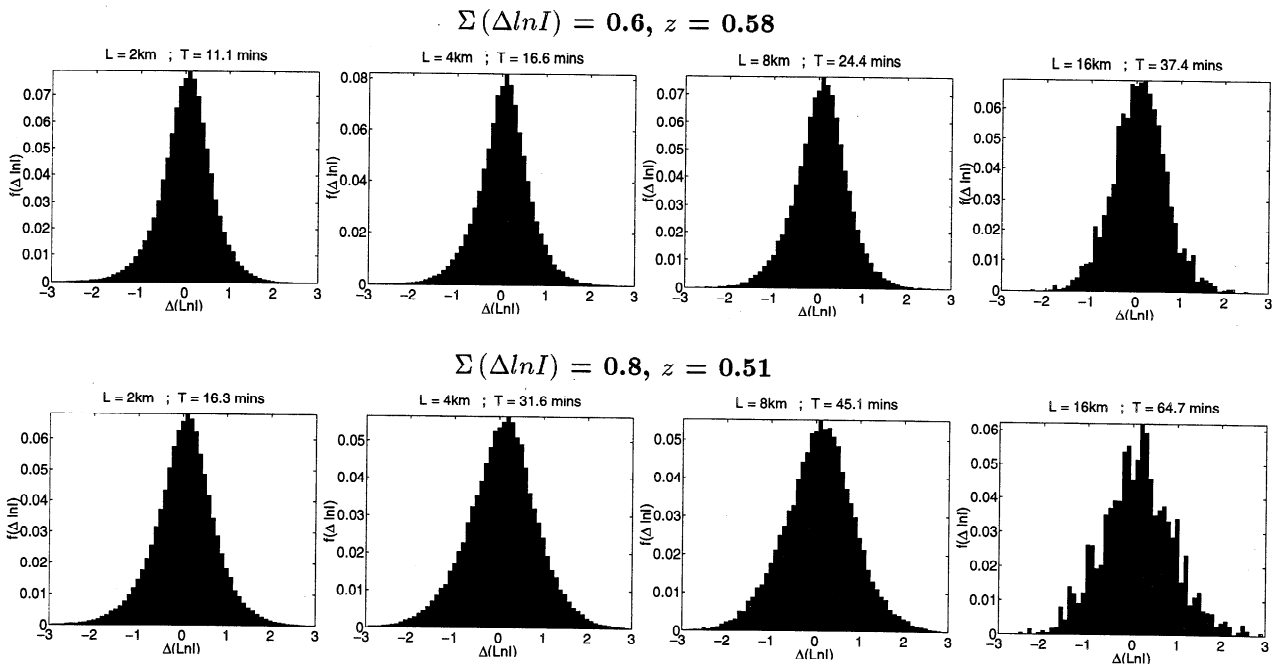

Figure 10. For region 1 of the storm of December 28, 1993: confirmation that the PDFs remain statistically invariant under the transformation t/L^z = constant. The top row shows PDFs for $\Sigma(\Delta \ln I) = 0.6$, $z = 0.58$ and pairs of (t, L) which satisfy t/L^z = constant (see Table 2). The bottom row shows the same for $\Sigma(\Delta \ln I) = 0.8$, $z = 0.51$. Similar result holds for $\Sigma(\Delta \ln I) = 0.7$, $z = 0.54$.

tically invariant with scale. In other words, if t and L change in such a way that t/L^z remains constant, the evolution of the fields remains statistically invariant (dynamic scaling). The value of the dynamic scaling exponent z was found to vary between 0.6 and 1.2, at least for the three analyzed storms which were convective rainy-season storms in Darwin, Australia. For example, a value of $z = 0.6$ would imply that the rate of change of an 8-times smaller feature is 3-times faster than the larger feature (since $t_2 = t_1 \times (L_2/8L_2)^{0.6} \approx 0.3t_2$). Although this type of relationship is not qualitatively surprising, the physical ground for such a scale-invariant

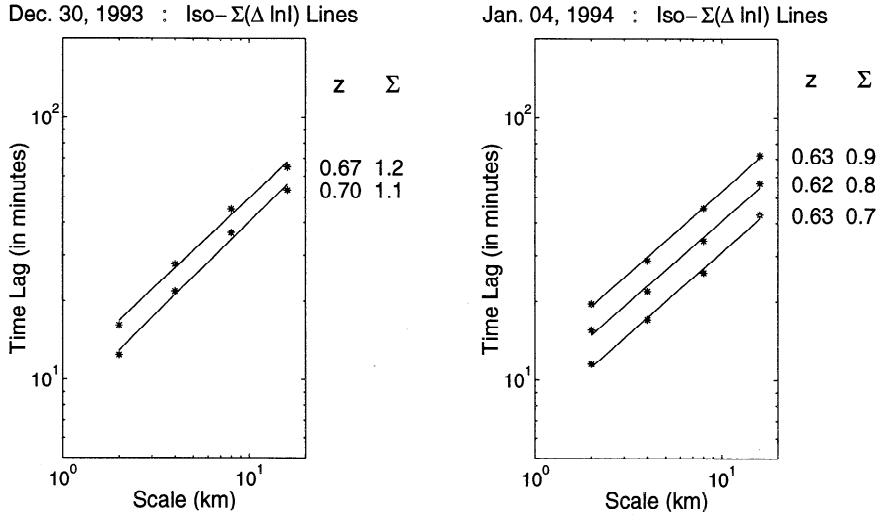

Figure 11. Plot illustrating the presence of dynamic scaling in the standard deviations of $\Delta \ln I$ for (a) region 1 of the storm of December 30, 1993 (left), and (b) region 1 of the storm of January 4, 1994, in Darwin, Australia (right). The log-log linear relationship between t and L for each value of $\Sigma(\Delta \ln I)$ given above supports the presence of dynamic scaling. For the left plot, the curves from top to bottom correspond to $\Sigma(\Delta \ln I) = 1.2$, z = 0.67 and $\Sigma(\Delta \ln I) = 1.1$, z = 0.7. Similarly, for the right-hand plot, from top to bottom, $\Sigma(\Delta \ln I) = 0.9$, z = 0.63; $\Sigma(\Delta \ln I) = 0.8$, z = 0.62; $\Sigma(\Delta \ln I) = 0.7$, z = 0.63.

space-time organization in rainfall is not immediately clear at this time. Further research is needed to address this issue.

It is noted that the scaling exponent z in our dynamic scaling approach bears a resemblance to the anisotropy parameter H of *Marsan et al.* [1996]. Specifically, it seems like there might exist a functional relation between z and H, namely, $z = 1 - H$. The value of H that they obtained from their analysis of observed radar rainfall data over the United States was $\approx$ -0.2, which matches the value of $z \approx 1.2$ that we obtained for a portion of one tropical Darwin storm presented here and also for several summertime midwestern convective storms analyzed by *Venugopal* [1999]. However, for several of the tropical storms analyzed herein as well as in some midwestern convective storms analyzed by *Venugopal* [1999], we found the value of z to be approximately 0.6 to 0.7. These values of z would correspond to values of H between 0.3 and 0.4 in the work of *Marsan et al.* [1996]. Such values were not reported in their study. Further analysis needs to be done to investigate the full range of possible z and H values for rainfall and also formally establish the aforementioned functional relation between z and H. In addition, it should be kept in mind that discrepancies in the ranges of z and H could potentially come from differences in the range of scales analyzed in the two studies (e.g., 2 to 6 km in our study versus > 8 km in their study).

It is speculated that z depends on physical properties of the storm environment, but no data are readily available to thoroughly investigate the exact nature of the relationship. For example, a possible parameter on which z might depend is the temporal change of the convective instability of the storm environment (∇CAPE). This variable is difficult to compute if sounding data are available only every 6 to 12 hours and only at one location within the storm coverage. We propose that future research on this issue needs to employ state-of-the-art numerical weather prediction models (mesoscale or storm-scale models) where physically consistent (assuming that we have confidence in the model physics) fields of precipitation and other environmental parameters can be produced and analyzed for (1) dynamic scaling and (2) relations of the dynamic scaling exponent with physical storm parameters.

The results reported in this study can be utilized to develop a space-time rainfall downscaling model which not only preserves the subgrid-scale spatial rainfall structure but also incorporates subgrid-scale temporal persistence. Such a model has been proposed in a companion paper by *Venugopal et al.* [1999] and has been shown successful in reproducing the subgrid space-time structure of rainfall given its large-scale space-time structure.

Acknowledgments. The material presented in this paper is based upon work supported by the joint GCIP-NOAA/NASA program under grant NAG8-1519 and partially by a NASA-TRMM grant NAG5-7715. The first author gratefully acknowledges support by a NASA Earth Systems Science Fellowship (NASA/NGT5-5014). We thank Robert Houze's group at the University of Washington for providing us with the Darwin data. Computer resources were provided by the Minnesota Supercomputer Institute. Many thanks to Alin Cârsteanu for his valuable comments. Two anonymous reviewers provided useful comments for improving the clarity of our presentation.

References

Cârsteanu, A., and E. Foufoula-Georgiou, Assessing dependence among weights in a multiplicative cascade model of temporal rainfall, *J. Geophys. Res., 101*(D21), 26,363-26,370, 1996.

Cârsteanu, A., Space-time rainfall modeling: Considerations of scaling and dynamics, Ph.D. thesis, Univ. of Minn., Minneapolis, 1997.

Czirok, A., E. Somfai, and T. Viscek, Experimental evidence for self-affine roughening in a micromodel of geomorphological evolution, *Phys. Rev. Lett., 71*(23), 2154-2157, 1993.

Foufoula-Georgiou, E., and W. Krajewski, Recent advances in rainfall modeling, estimation and forecasting, *U.S Nat. Rep., Int. Union Geod. Geophys., 1991-1994, Contrib. Hydrol.*, 1995.

Gupta, V., and E. Waymire, Multiscaling properties of spatial rainfall in river flow distributions, *J. Geophys. Res., 95*(D3), 1999-2009, 1990.

Kardar, M., G. Parisi, and Y. Zhang, Dynamic scaling of growing interfaces, *Phys. Rev. Lett, 56*, 889-892, 1986.

Kedem, B., L. S. Chiu, and G. R. North, Estimation of mean rainrate: Application to satellite observations, *J. Geophys. Res., 95*(D2), 1965-1972, 1990.

Kumar, P., and E. Foufoula-Georgiou, A multicomponent decomposition of spatial rainfall fields, 1, Segregation of large and small-scale features using wavelet transforms, *Water Resour. Res., 29*(8), 2515-2532, 1993a.

Kumar, P., and E. Foufoula-Georgiou, A multicomponent decomposition of spatial rainfall fields, 2, Self-similarity in fluctuations, *Water Resour. Res., 29*(8), 2533-2544, 1993b.

Kumar, P., Role of coherent structures in the stochastic-dynamic variability of precipitation, *J. Geophys. Res., 101*(D21), 26,393-26,404, 1996.

Marsan, D., D. Schertzer, and S. Lovejoy, Causal space-time multifractal processes: Predictability and forecasting of rain fields, *J. Geophys. Res., 101*(D21), 26,333-26,346, 1996.

Olsson, J., J. Niemczynowicz, and R. Berndtsson, Fractal analysis of high resolution rainfall time series, *J. Geophys. Res., 98*(D12), 23,265-23,274, 1993.

Over, T.M., and V. K. Gupta, Statistical analysis of mesoscale rainfall: Dependence of a random cascade generator on large-scale forcing, *J. Appl. Meteorol., 33*(12), 1526-1542, 1994.

Over, T.M., and V. K. Gupta, A space-time theory of mesoscale rainfall using random cascades, *J. Geophys. Res., 101*(D21), 26,319-26,331, 1996.

Perica, S., and E. Foufoula-Georgiou, Linkage of scaling and thermodynamic parameters of rainfall: Results from midlatitude mesoscale convective systems, *J. Geophys. Res., 101*(D3), 7431-7448, 1996.

Schertzer, D., and S. Lovejoy, Physical modeling and analysis of rain and clouds by anisotropic scaling multiplicative processes, *J. Geophys. Res., 92*(D8), 9693-9714, 1987.

Svensson, C., J. Olsson, and R. Berndtsson, Multifractal properties of daily rainfall in two different climates, *Water Resour. Res., 32*(8), 2463-2472, 1996.

Tessier, Y., S. Lovejoy, and D. Schertzer, Universal multifractals: Theory and observation for rain and clouds, *J. Appl. Meteorol., 32*(2), 223-250, 1993.

Veneziano, D., R. L. Bras, and J. D. Niemann, Nonlinearity and self-similarity of rainfall in time and a stochastic model, *J. Geophys. Res., 101*(D21), 26,371-26,392, 1996.

Venugopal, V., Spatio-temporal organization and space-time downscaling of precipitation fields, Ph.D. thesis, Univ. of Minn., Minneapolis, 1999.

Venugopal, V., and E. Foufoula-Georgiou, Energy decomposition of rainfall in the time-frequency-scale domain using wavelet packets, *J. Hydrol., 187*, 3-27, 1996.

Venugopal, V., E. Foufoula-Georgiou, and V. Sapozhnikov, A space-time downscaling model for rainfall, *J. Geophys. Res.*, in press, 1999.

Zawadzki, I., Statistical properties of precipitation patterns, *J. Appl. Meteorol., 12*, 459-472, 1973.

V. Venugopal, Center for Ocean-Land-Atmosphere Studies, 4041 Powder Mill Road, Suite 302, Calverton, MD 20705. (e-mail: venu@cola.iges.org)

Efi Foufoula-Georgiou and Victor Sapozhnikov, St. Anthony Falls Laboratory, University of Minnesota, Mississippi River at Third Avenue SE, Minneapolis, MN 55414. (e-mail: efi@mykonos.safhl.umn.edu; victor@mykonos.safhl.umn.edu)

(Received October 2, 1998; revised April 21, 1999; accepted June 4, 1999.)